ELSEVIER

Wear 249 (2002) 943–950

WEAR

www.elsevier.com/locate/wear

# Waterjet and abrasive waterjet surface treatment of titanium: a comparison of surface texture and residual stress

D. Arola [a,*], M.L. McCain [a], S. Kunaporn [b], M. Ramulu [b]

[a] *Department of Mechanical Engineering, University of Maryland Baltimore County, 1000 Hilltop Circle, Baltimore, MD 21250, USA*

[b] *Department of Mechanical Engineering, University of Washington, Box 352600, Seattle, WA 98195, USA*

Received 2 February 2001; accepted 4 July 2001

**Abstract**

In this study, commercially pure titanium (cpTi) and a titanium alloy (Ti6Al4V) were subjected to waterjet (WJ) peening and abrasive waterjet (AWJ) peening surface treatments. The texture and in-plane biaxial residual stress of the treated surfaces were quantified using contact profilometry and X-ray diffraction, respectively. Regardless of the specific process conditions, the surface residual stresses resulting from WJ and AWJ peening of both materials were compressive. Residual stresses in the Ti6Al4V ranging $-400 \leq \sigma \leq -30$ MPa, whereas stresses in the cpTi treated with the same conditions ranging $-200 \leq \sigma \leq -60$ MPa. Residual stresses resulting from WJ peening increased with the WJ pressure whereas those resulting from AWJ peening decreased with an increase in both jet pressure and abrasive size. The surface roughness of the metals did not change appreciably with WJ treatment, but AWJ peening resulted in a significant increase in roughness. Therefore, AWJ peening may serve as a new method for introducing compressive residual stresses in engineering components that also require rough surfaces. 

*Keywords:* Residual stress; Shot peening; Surface integrity; Waterjet

## 1. Introduction

The surface roughness and surface integrity resulting from net-shape processing may be detrimental to the fatigue-life and corrosion resistance of engineering components. Of critical concern are stress concentrations posed by the surface topography, residual stresses caused by localized deformation or thermal transformations, and alterations in the surface hardness that result from processing [1]. Components that require superior fatigue strength and/or resistance to stress corrosion cracking are often subjected to secondary manufacturing processes.

Secondary processes are utilized to minimize the component surface roughness and/or introduce a compressive near-surface residual stress. The most common methods enrolled for fatigue-life improvement include shot peening [2–4], roller burnishing [5–7], and abrasive finishing [8]. Laser peening [9,10] and waterjet (WJ) peening [11–16] have also recently emerged as viable alternatives to conventional methods of surface treatment.

Although, beneficial for components that require smooth surfaces, existing methods of secondary processing are not feasible for components that simultaneously require fatigue strength and rough surface texture. One such component that requires these properties are metal prosthetic devices used in cementless total joint replacements [17,18]. Any surface that must maintain adhesion with a second substrate under fatigue loading is subjected to these same requirements. Although, plasma spray and deposition based technologies can be used in the development of a rough surface texture, they seldom offer, or are able to maintain, high fatigue strength.

The objective of this study was to examine and compare the surface topography and in-plane residual stress that results from two different non-traditional surface treatment processes. Both processes utilized a high pressure WJ that is targeted on the substrate at normal angles of jet impingement; one of the processes utilized a pure WJ (i.e. WJ peening) and the second was comprised of a WJ laden with abrasives (abrasive waterjet (AWJ) peening). A secondary objective was to evaluate the use of AWJ peening as a surface treatment process capable of providing a rough surface texture and near-surface compressive residual stress.

* Corresponding author. Tel.: +1-410-455-3300; fax: +1-410-455-1052.
*E-mail address:* darola@engr.umbc.edu (D. Arola).

0043-1648/01/$ – see front matter 
PII: S0043-1648(01)00826-2

Table 1
Treatment conditions used for WJ and AWJ peening of the titanium plates

| Experiment | Pressure (MPa) | Abrasive (mesh no.) | Standoff (m) | Traverse speed (m/min) |
|---|---|---|---|---|
| AWJ | | | | |
| 1 | 280 | 50 | 0.15 | 3.81 |
| 2 | 280 | 80 | 0.15 | 3.81 |
| 3 | 280 | 120 | 0.15 | 3.81 |
| 4 | 210 | 50 | 0.15 | 3.81 |
| 5 | 210 | 80 | 0.15 | 3.81 |
| 6 | 210 | 120 | 0.15 | 3.81 |
| 7 | 140 | 50 | 0.15 | 3.81 |
| 8 | 140 | 80 | 0.15 | 3.81 |
| 9 | 140 | 120 | 0.15 | 3.81 |
| 10 | 80 | 50 | 0.15 | 3.81 |
| 11 | 80 | 80 | 0.15 | 3.81 |
| 12 | 80 | 120 | 0.15 | 3.81 |
| WJ | | | | |
| 13 | 280 | None | 0.15 | 3.81 |
| 14 | 210 | None | 0.15 | 3.81 |
| 15 | 140 | None | 0.15 | 3.81 |

## 2. Materials and methods

### 2.1. Material

Grade 2 commercially pure titanium (cpTi) and Grade 5 titanium alloy of composition Ti6Al4V were utilized in this investigation. The cpTi and Ti6Al4V were obtained in plate form with 3.2 and 6.4 mm thickness, respectively. The cpTi has an elastic modulus of 104 GPa, yield and ultimate strength of 330 and 500 MPa, respectively, and elongation of 24%. The Ti6Al4V has an elastic modulus of 114 GPa, yield and ultimate strength of 900 and 980 MPa, respectively, and 16% elongation.

### 2.2. Equipment and procedures

An AWJ [1] was used for all surface treatments of the titanium samples. The WJ system used in this study is capable of developing jet pressures up to 300 MPa and has a working envelope of 0.7 m × 1.3 m. A nozzle assembly with 0.30 mm diameter sapphire jewel and tungsten carbide focusing tube with 0.9 mm diameter and 89 mm length was used for all WJ and AWJ surface treatments performed. Garnet abrasives were used for all the AWJ peening experiments.

AWJ peening of the two metals was conducted with 12 different parametric conditions as listed in Table 1. Four jet pressures ranging from 70 to 280 MPa and three levels of abrasive mesh (#50, #80, and #120 mesh) were used. In addition, WJ peening was conducted with each of the titanium substrates over three jet pressures. The standoff distance for both AWJ and WJ peening was held constant in this preliminary study at 0.15 m, which resulted in a jet treatment diameter at impingement of approximately

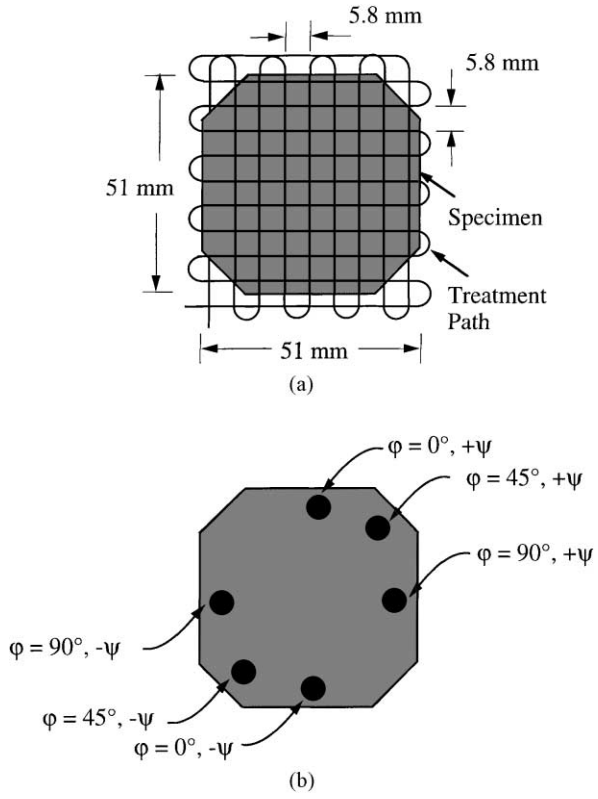


Fig. 1. Specimens, surface treatment, and location of diffraction measurements. (a) Surface treatment pattern and specimen size; (b) X-ray diffraction measurement scheme.

16 mm. Peening of the cpTi and Ti6Al4V was conducted at normal angles of jet impingement using a traverse pattern as shown in Fig. 1(a). A cross-hatch pattern was used to insure full treatment of the entire specimen surface area and to minimize macroscopic surface variations that may result from the combined deformation/erosion process. Both processes were conducted using a single-pass treatment (no replication) with a traverse speed of 3.81 m/min. Following treatment, specimens representative of each surface were sectioned from the plates using the AWJ for further analysis.

Surface profiles of the cpTi and Ti6Al4V samples were obtained using a stylus surface profilometer [2] using a traverse length of 4.8 mm and cutoff length of 0.8 mm. A skidless contact probe with 10 μm diameter was used for all measurements. Surface profiles were used in calculating the arithmetic average roughness ($R_a$), peak to valley height ($R_v$), and ten point roughness ($R_z$), according to ANSI B46.1. In addition to the standard roughness parameters, the material ratio curve was used in calculating the core $R_k$ parameters ($R_k$, $R_{vk}$, and $R_{pk}$) according to DIN 4776. An evaluation of the microscopic features of the treated surfaces was conducted with a Jeol JSM T-35 scanning electron microscope (SEM).

[1] Model 2652, OMAX Corp., Auburn, WA.

[2] Model T8000 Profilometer, Hommel, New Britain, CT.

A residual stress analysis of the surfaces was conducted with an X-ray diffractometer[3] using Cu Kα radiation with a wavelength (λ) of 1.54060 Å and beam width of 0.5 mm at 40 kV and 30 mA. Peak intensities of the diffraction patterns were recorded at $\phi$ angles of 0°, 45° and 90° with $\pm\psi$ tilts of 0°, 17.46°, 25.18°, 31.37° and 36.99°. Thus, the surface residual stress in each specimen was determined from a total of 30 diffraction measurements. Negative $\psi$ tilts were conducted with pseudo-negative $\psi$ angles according to the measurement scheme shown in Fig. 1(b). All peak intensities were corrected for Lorentz polarization, absorption, and background intensity using a linear correction. Peak positions of the diffraction patterns were found from the center of gravity and used to determine the lattice plane spacing according to Bragg's law [19]. The magnitude of biaxial residual stress was determined using the $\sin^2\psi$ method of analysis, which provides an average value of the in-plane stress distribution over the depth of X-ray penetration [19]. Absorption coefficients for the cpTi and Ti6Al4V were determined to be 912.8 and 902.5 $cm^{-1}$ which correspond to an X-ray penetration depth (for 99% absorption) of 12.0 and 12.1 μm, respectively.

The diffracted beam from the AWJ peened samples was found to suffer from a significant loss in beam intensity during the X-ray analysis. As all the AWJ peened specimens exhibited this characteristic, it was uncertain whether the reduction in beam intensity was due to an increase in surface roughness or changes in the surface chemistry that resulted from abrasive debris. Therefore, an elemental analysis of the Ti6Al4V surface was conducted using a Jeol JSM-840A SEM with a KEVEX SIGMA Level 4 energy dispersive spectrometer (EDS) and quantum detector. The system was used to perform an X-ray microanalysis in which differences in material conductivity on the Ti6Al4V surface (as a result of elemental composition) are detected and used to provide high resolution contrast images. An image analysis software (GMBH Analysis 2.2) was used to translate contrast differentials into quantitative data and an image processing software was used to calculate the concentration of garnet abrasives remaining on representative surfaces after treatment.

## 3. Results

AWJ and pure WJ peening of the titanium samples was conducted over a range of parametric conditions as described in Table 1. A macroscopic examination of the specimens indicated that the surface topography resulting from AWJ peening was highly dependent on the operating conditions. However, there were minimal differences in the macroscopic features of the WJ peened titanium resulting from surface treatment, regardless of the process parameters.

[3] Model 1830 Generator and PW 1710/00 Diffraction Control Unit, Phillips.

### 3.1. Surface topography

A representative surface profile resulting from AWJ peening of the cpTi and Ti6Al4V is shown in Fig. 2(a) and (b). The profiles in this figure were obtained from the surface of Specimen 1 treated with a jet pressure of 280 MPa and #50 mesh (Table 1). Surface roughness parameters for the cpTi and Ti6Al4V specimens were calculated from the respective surface profiles and are listed in Tables 2 and 3, respectively. Based on a comparison of the standard roughness parameters for each material, the surface texture resulting from AWJ peening was primarily dependent on the treatment condition, not the material. The highest average surface roughness ($R_a$) of the AWJ peened specimens resulted from treatment with the highest jet pressure and largest abrasive mesh (Specimen 1) as evident from Tables 2 and 3. Although, the surface roughness of the metals did increase with WJ peening, the changes were far less significant than those resulting from AWJ peening. The largest surface roughness resulting from WJ peening of the two metals occurred in treatment of the cpTi as expected from the comparatively low yield strength. However, the largest change in surface roughness resulting from WJ

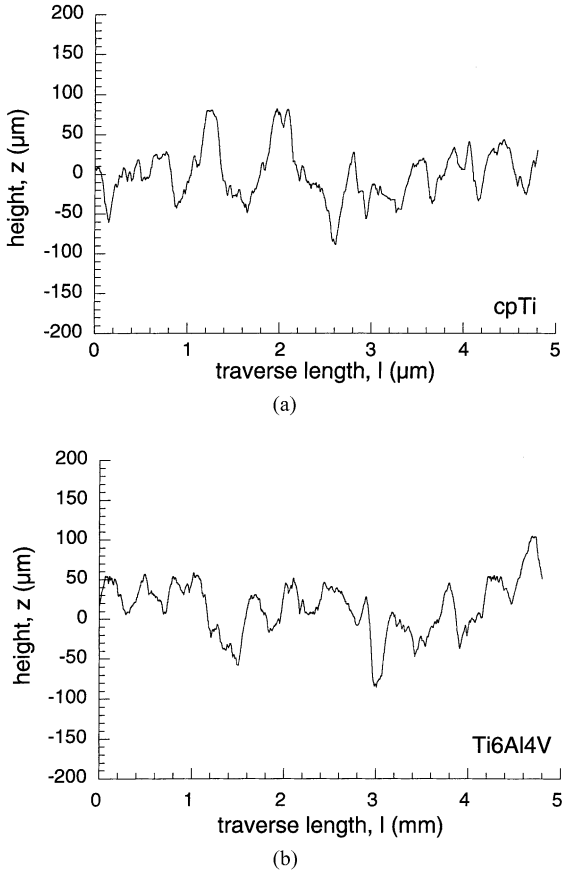


Fig. 2. Typical surface profiles of the AWJ peened titanium. The samples were treated with #50 abrasives and jet pressure of 280 MPa. (a) AWJ peened cpTi; (b) AWJ peened Ti6Al4V.

Table 2
Surface roughness resulting from treatment of the cpTi

| Specimen | $R_a$ (μm) | $R_z$ (μm) | $R_y$ (μm) | $R_k$ (μm) | $R_{pk}$ (μm) | $R_{vk}$ (μm) |
|---|---|---|---|---|---|---|
| 1 | 15.5 | 79.6 | 120.9 | 51.9 | 21.2 | 21.7 |
| 2 | 11.7 | 63.9 | 85.1 | 41.6 | 12.1 | 15.0 |
| 3 | 8.5 | 49.3 | 57.3 | 27.3 | 9.9 | 9.9 |
| 4 | 13.5 | 65.9 | 88.9 | 42.5 | 9.3 | 20.8 |
| 5 | 11.3 | 59.5 | 73.4 | 39.8 | 7.1 | 14.4 |
| 6 | 7.9 | 45.1 | 53.7 | 26.8 | 8.1 | 9.2 |
| 7 | 11.3 | 58.5 | 72.7 | 35.8 | 13.6 | 12.7 |
| 8 | 7.3 | 46.8 | 59.3 | 22.6 | 10.6 | 11.7 |
| 9 | 5.5 | 36.2 | 51.7 | 16.3 | 7.5 | 9.6 |
| 10 | 8.0 | 47.0 | 61.5 | 24.3 | 10.4 | 12.6 |
| 11 | 6.0 | 37.0 | 45.6 | 18.3 | 7.1 | 7.9 |
| 12 | 4.1 | 26.9 | 35.4 | 13.1 | 5.5 | 5.2 |
| 13 | 3.7 | 18.1 | 21.6 | 12.8 | 2.1 | 4.3 |
| 14 | 3.3 | 17.4 | 20.0 | 10.7 | 2.8 | 3.8 |
| 15 | 3.2 | 16.1 | 19.4 | 11.1 | 2.5 | 2.9 |
| Substrate | 2.9 | 14.3 | 18.2 | 9.6 | 2.3 | 3.2 |

Table 3
Surface roughness resulting from treatment of the Ti6Al4V

| Specimen | $R_a$ (μm) | $R_z$ (μm) | $R_y$ (μm) | $R_k$ (μm) | $R_{pk}$ (μm) | $R_{vk}$ (μm) |
|---|---|---|---|---|---|---|
| 1 | 14.2 | 76.7 | 95.8 | 46.9 | 20.9 | 21.8 |
| 2 | 11.0 | 60.8 | 84.5 | 34.9 | 16.2 | 16.7 |
| 3 | 7.6 | 42.6 | 54.2 | 26.4 | 10.5 | 8.1 |
| 4 | 12.2 | 64.5 | 86.4 | 40.2 | 16.8 | 15.6 |
| 5 | 9.4 | 51.8 | 74.6 | 31.7 | 12.6 | 11.1 |
| 6 | 6.3 | 35.9 | 43.7 | 20.8 | 7.6 | 7.0 |
| 7 | 10.1 | 53.8 | 69.7 | 31.6 | 10.8 | 15.4 |
| 8 | 8.9 | 49.4 | 61.1 | 28.3 | 7.4 | 13.9 |
| 9 | 4.7 | 30.3 | 35.5 | 14.4 | 5.0 | 7.7 |
| 10 | 7.6 | 44.5 | 59.0 | 26.1 | 7.3 | 13.9 |
| 11 | 5.7 | 33.9 | 44.5 | 19.2 | 5.7 | 7.5 |
| 12 | 3.6 | 21.9 | 30.0 | 10.9 | 3.5 | 7.1 |
| 13 | 2.4 | 14.6 | 17.9 | 7.7 | 1.4 | 7.0 |
| 14 | 2.2 | 14.8 | 23.0 | 6.2 | 2.4 | 6.4 |
| 15 | 1.0 | 6.0 | 8.6 | 3.0 | 1.0 | 2.2 |
| Substrate | 0.9 | 5.9 | 9.8 | 2.4 | 1.0 | 1.8 |

peening occurred in treatment of the Ti6Al4V due to the low original substrate roughness ($R_a = 0.9\,\mu m$, Table 3).

### 3.2. Residual stress

Residual stresses resulting from WJ and AWJ peening of the titanium specimens were computed using the $\sin^2\psi$ method of analysis. The biaxial in-plane residual stresses determined for both the WJ and AWJ peened cpTi and Ti6Al4V are listed in Table 4. It was found that the residual stresses resulting from all conditions of surface treatment in this study were compressive; the magnitude of stress in the cpTi ranged from 60 to over 200 MPa while the residual stress within the Ti6Al4V ranged from near 30 MPa to over 400 MPa. Similar to the observed changes in surface texture, residual stresses in both materials were strongly dependent on the treatment conditions. The largest compressive residual stress resulting from AWJ peening of the two metals was treated with a jet pressure of 70 MPa and #120 mesh abrasives. The largest residual stress resulting from WJ peening of the two metals was near 180 MPa and resulted at the highest jet pressure. Note that, the biaxial stresses presented in Table 4 represent the average stress determined over the depth of X-ray penetration. Subsurface residual stress gradients resulting from AWJ peening are also a significant element of the surface integrity and will be identified in future studies.

## 4. Discussion

A comparison of the surface texture and residual stress resulting from WJ and AWJ peening of the metals clearly differentiated the two surface treatment processes. The surface roughness resulting from AWJ peening of the cpTi and Ti6Al4V was significantly larger than that resulting from WJ peening and increased with jet pressure and abrasive size.

Table 4
Compressive residual stress resulting from WJ and AWJ peening of the titanium

| Experiment | Pressure (MPa) | Abrasive (mesh no.) | cpTi stress (MPa) | Ti6Al4V stress (MPa) | $\sigma_{cpTi}/\sigma_{Ti6Al4V}$ (MPa/MPa) |
|---|---|---|---|---|---|
| 1 | 280 | 50 | 103 ± 30 | 88 ± 55 | 1.2 |
| 2 | 280 | 80 | 87 ± 25 | 128 ± 57 | 0.7 |
| 3 | 280 | 120 | 124 ± 26 | 196 ± 39 | 0.6 |
| 4 | 210 | 50 | 98 ± 30 | 142 ± 41 | 0.7 |
| 5 | 210 | 80 | 115 ± 30 | 181 ± 56 | 0.6 |
| 6 | 210 | 120 | 149 ± 33 | 186 ± 56 | 0.8 |
| 7 | 140 | 50 | 118 ± 32 | 186 ± 57 | 0.6 |
| 8 | 140 | 80 | 168 ± 24 | 184 ± 47 | 0.9 |
| 9 | 140 | 120 | 175 ± 22 | 318 ± 36 | 0.6 |
| 10 | 70 | 50 | 144 ± 23 | 266 ± 55 | 0.5 |
| 11 | 70 | 80 | 178 ± 32 | 240 ± 44 | 0.7 |
| 12 | 70 | 120 | 193 ± 29 | 353 ± 56 | 0.5 |
| 13 | 280 | None | 163 ± 24 | 118 ± 36 | 1.4 |
| 14 | 210 | None | 124 ± 28 | 93 ± 40 | 1.3 |
| 15 | 140 | None | 93 ± 27 | 85 ± 38 | 1.1 |

In addition, the surface texture resulting from AWJ peening of the cpTi was equivalent to that resulting from treatment of the Ti6Al4V with the same conditions as evident from a comparison of the surface roughness parameters in Tables 2 and 3. In comparison to changes in surface texture invoked from AWJ peening, there was only a mild increase in surface roughness of the metals with an increase in WJ peening pressure.

AWJ peening invoked a combination of erosion and localized plastic deformation as a result of abrasive particle impact at nearly orthogonal particle attack angles. Abrasive indentations on the titanium surfaces would undoubtedly contribute to the fatigue-life of treated components, especially through the radius of curvature of dominant profile valley radii. The smallest profile valley radii distinguished from the AWJ peened cpTi and Ti6Al4V surfaces presented in Fig. 2 are shown in Fig. 3(a) and (b), respectively. Although, there was no definitive trend in the profile valley radii of the AWJ peened metals, surfaces treated with #50 abrasives and higher jet pressures (e.g. treatment combinations 1 and 4 of Table 1) appeared to exhibit the smallest valley radii of all surfaces examined [18]. For the surfaces

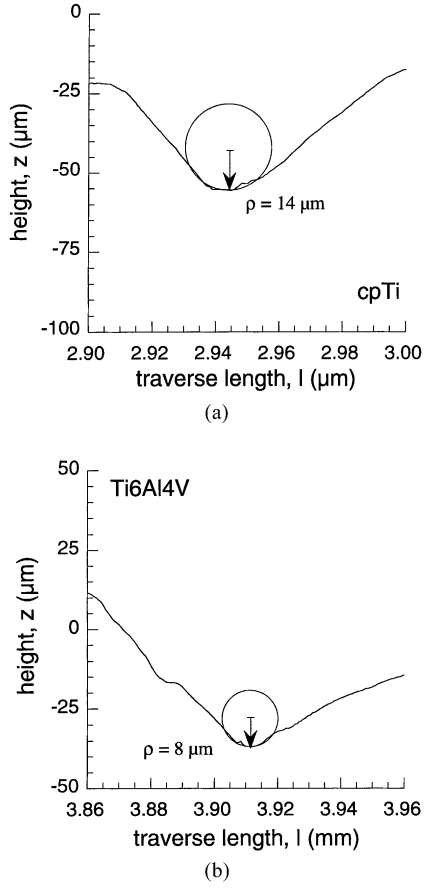


Fig. 3. Minimum profile valley radii obtained from surface profiles of the AWJ peened specimens. The samples in these figures were treated with #50 abrasives and jet pressure of 280 MPa. (a) AWJ peened cpTi from Fig. 2a; (b) AWJ peened Ti6Al4V from Fig. 2(b).

treated with lower jet pressures, there was no trend evident between the profile valley radii and treatment parameters. It is expected that the increase in kinetic energy achieved with use of large abrasives and high jet pressures results in more substantial single particle impact and facilitates the development of distinct indentations with small valley radii. Nevertheless, additional research is required to understand the relationship between treatment parameters, abrasive particle shape, and the resulting profile valley radii.

Although, the surface texture resulting from AWJ peening was dependent on the treatment conditions, microscopic features of the specimens appeared relatively independent of the process parameters. During the microscopic analysis, garnet abrasives were found partially impregnated within both the AWJ peened cpTi and Ti6Al4V surfaces. Abrasive residue has also been documented on substrates subjected to grit blasting [20,21]. Note that, the abrasive particles located on the AWJ peened surfaces appeared to be a combination of whole abrasives and fractured residue. A micrograph highlighting abrasives impregnated within a Ti6Al4V surface is shown in Fig. 4(a). Abrasives have also been found impregnated in the surface of metals subjected to AWJ machining in which the particle attack angle is much more acute [15,22]. EDS was used to highlight abrasive particles in the surface of selected specimens and obtain estimates of the abrasive particle concentration covering the treatment surface. An example of abrasives distinguished using this approach in the surface of the AWJ peened sample in Fig. 4(a) is shown in Fig. 4(b). Approximately 7% of the total surface area was covered with abrasive particles while selected areas were found to exhibit much higher concentrations (e.g. Fig. 4(c)). Although, the SEM and EDS analysis were not conducted with all specimens, the concentration of abrasives appeared to increase with increasing jet pressure and smaller abrasive particles. Furthermore, a higher concentration of abrasives were found deposited in the AWJ peened cpTi surface in comparison to that of the Ti6Al4V. The larger concentration of abrasives found in the cpTi is undoubtedly attributed to the lower yield strength of this material and opportunity for deposition through extensive plastic deformation.

Residual stresses resulting from AWJ machining of metals have been shown to be compressive, and relatively insensitive to the cutting condition [23]. In contrast, residual stresses within the titanium resulting from WJ and AWJ peening were largely dependent on the treatment conditions as evident from the range in stress reported in Table 4. The influence of jet pressure and abrasive mesh number on residual stresses in the cpTi and Ti6Al4V specimens is shown in Fig. 5(a) and (b). The magnitude of compressive residual stress in both materials increased with a decrease in abrasive size and jet pressure. An increase in jet pressure and the use of larger abrasives promoted an increase in the jet energy available for hydrodynamic erosion. Consequently, material removal allowed near-surface stress relief of the surface layers and resulted in a reduction in the magnitude of compressive stress. Residual stresses resulting from WJ

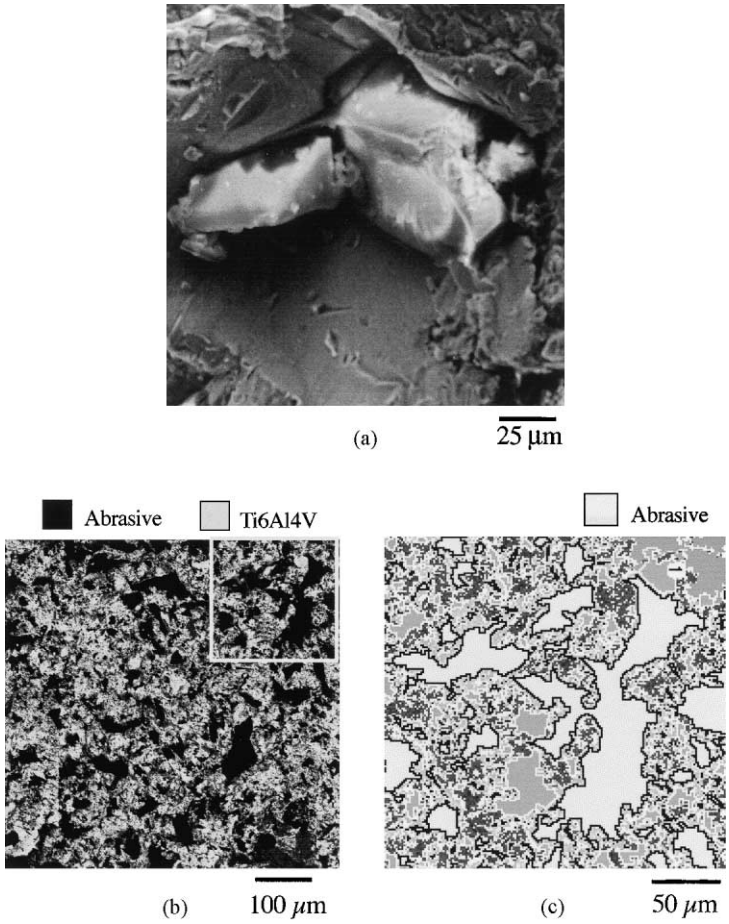


Fig. 4. Abrasive deposition in the Ti6Al4V resulting from AWJ peening of the Ti6Al4V. The sample was treated with #80 abrasives and jet pressure of 280 MPa (experiment 2 of Table 1). (a) Garnet abrasives in the Ti6Al4V surface; (b) abrasive particles isolated using EDS (highlight shown in (c)); (c) abrasive particles outlined using image analysis. Abrasives represent 17.5% of the selected treatment surface area.

peening of both metals increased with treatment pressure as shown in Fig. 5(c). The absence of material removal in WJ peening resulted in an increase in the near-surface deformation with increasing pressure. Nevertheless, residual stresses within both materials that resulted from AWJ peening exceeded those that resulted from WJ peening at the same jet pressure.

As evident from Table 4, the residual stress resulting from AWJ peening of the cpTi ($\sigma_{\text{cpTi}}$) was generally lower than that resulting from treatment of the Ti6Al4V ($\sigma_{\text{Ti6Al4V}}$) using the same conditions. However, contrary to the existing understanding of surface treatments and residual stresses derived from shot peening, residual stresses resulting from WJ peening of the cpTi were greater than obtained from treatment of the Ti6Al4V. The comparatively high yield strength of the Ti6Al4V and deformable nature of the pure WJ droplets limited the degree of near-surface plastic deformation that occurred during WJ peening of the Ti6Al4V. It appears that the lower yield strength of the cpTi enabled more extensive near-surface deformation during WJ peening and resulted in a larger compressive residual stress. The comparatively low yield strength of the cpTi also allowed erosion to occur more extensively during WJ peening, than in treatment of the Ti6Al4V, as evident from the larger surface roughness of the WJ peened cpTi samples (Table 4).

Based on the preliminary results, it would appear that WJ peening would be less effective in the surface treatment of hard metals or those that exhibit high yield strength and/or hardness. However, WJ peening has been reported as an effective method of treatment for cutting tools and other high strength materials [12,14,24]. The WJ pressures used for treatment in these previous investigations were significantly higher than those used for the comparative study. In this study, the treatment conditions for both processes were selected to maintain consistency and comply with the machine limits. As such, the conditions for both processes were only differentiated by the addition of abrasives in AWJ peening. Therefore, further improvement in the magnitude of compressive residual stress resulting from WJ peening would likely result from higher jet pressures than those used in this investigation. Furthermore, WJ peening may be more effective as a multi-pass treatment process whereas results from this study were achieved from a single treatment. AWJ peening could serves as a viable process of surface treatment

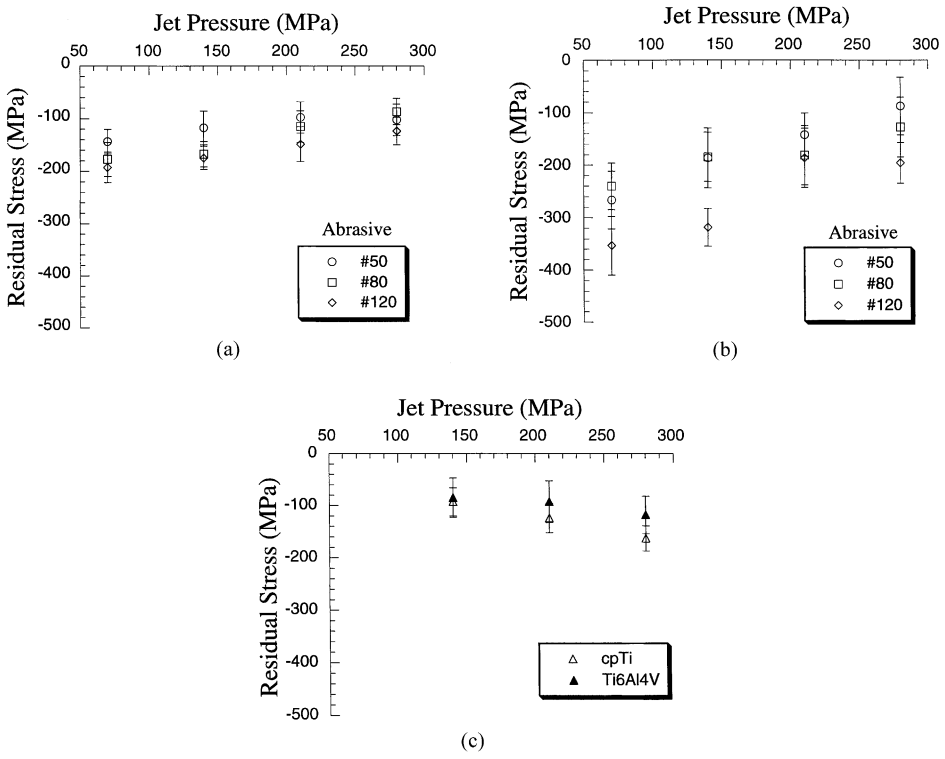


Fig. 5. Influence of treatment parameters on the residual stress. (a) AWJ peening of the cpTi; (b) AWJ peening of the Ti6Al4V; (c) WJ peening of the cpTi and Ti6Al4V.

where rough surface texture and compressive residual stresses were desired. If the component fatigue strength were of concern, then proper abrasive selection (including appropriate size and shape) would be necessary to minimize abrasives impregnated within the substrate and to control profile valley radii of surface indentations. Evaluations of grit blasting have revealed that grit residue remaining on treated surfaces was a function of impingement angle and was a maximum for orthogonal impingement (90°) [20]. Therefore, the concentration of abrasives impregnated within the substrate that results from AWJ peening may reduce through changes in impingement angle. Our future work will focus on the applications of AWJ peening and the ability to simultaneously control the surface texture, residual stress, and concentration of impregnated abrasives that result from this process as a function of the treatment parameters.

## 5. Conclusions

An experimental study comprised of WJ and AWJ peening of cpTi and Ti6Al4V was performed. A comparison of the surface texture and surface integrity resulting from each method of processing was conducted. The metals were processed over a selected range in treatment parameters and the surfaces were evaluated in terms of the resulting surface roughness and magnitude of in-plane biaxial residual stress. Based on results from this study, the following conclusions were drawn:

1. AWJ peening invoked a significant increase in the surface roughness of both metals. The maximum average surface roughness resulting from treatment was 15 μm and resulted from AWJ peening with the largest garnet abrasive (#50) and highest jet pressure (280 MPa). In addition, garnet abrasives were found impregnated within the AWJ peened surfaces of both metals.
2. Both WJ and AWJ peening introduced compressive residual stresses in the metal surfaces. The maximum compressive residual stress resulting from WJ and AWJ peening was approximately 180 and 400 MPa, respectively.
3. Residual stresses within the Ti6Al4V resulting from AWJ peening were greater than those that developed in the cpTi subjected to the same treatment conditions. However, residual stresses resulting from WJ peening of the cpTi were greater than those that developed in the Ti6Al4V.

## Acknowledgements

The first author gratefully acknowledges partial support from the OMAX Corporation in the form of an equipment grant. The authors also acknowledge Victor Champagne and

Daniel Snoha of the Army Research Laboratory at Aberdeen Proving Ground for performing the EDS analysis.

## References

[1] E. Zahavi, V. Torbilo, Fatigue Design. Life Expectancy of Machine Parts, CRC Press, Boca Raton, FL, 1996, pp. 239–257.
[2] J.O. Almen, P.H. Black, Residual Stresses and Fatigue in Metals, McGraw Hill, New York, 1963.
[3] D. Kirk, Shot Peening, Aircraft Eng. Aerospace Technol. 71 (4) (1999) 349–361.
[4] M. Kobayashi, T. Matsui, Y. Murakami, Mechanism of creation of compressive residual stress by shot peening, Int. J. Fatigue 20 (5) (1998) 351–357.
[5] M.H. El-Axir, Investigation into roller burnishing, Int. J. Machine Tools Manufac. 40 (11) (2000) 1603–1617.
[6] A.M. Hassan, A.S. Al-Bsharat, Influence of burnishing process of surface roughness, hardness and microstructure of some non-ferrous metals, Wear 199 (1996) 1–8.
[7] F. Klocke, J. Liermann, Roller burnishing of hard turned surfaces, Int. J. Machine Tools Manufact. 38 (5/6) (1998) 419–423.
[8] T.K. Puthanangady, S. Malkin, Experimental investigation of the superfinishing process, Wear 185 (1/2) (1995) 173–182.
[9] C.B. Dane, L.A. Hackel, J. Daly, J. Harrisson, Laser peening of metals — enabling laser technology, in: Proceedings of the Materials Research Society, Vol. 499, 1–4 December 1997, 1998, pp. 73–85.
[10] P. Peyre, X. Scherpereel, L. Berthe, C. Carboni, R. Fabbro, G. Beranger, C. Lemaitre, Surface modifications induced in 316l steel by laser peening and shot-peening. Influence on pitting corrosion resistance, Mater. Sci. Eng. A: Struct. Mater.: Properties, Microstruct. Process. 280 (2) (2000) 294–302.
[11] H.K. Tonshoff, F. Kroos, M. Hartmann, Water peening — an advanced application of waterjet technology, in: Proceedings of the 8th American Waterjet Conference, Houston, TX, 26–29 August 1995, pp. 473–486.
[12] H.K. Tonshoff, F. Kroos, C. Marzenell, High-pressure water peening — a new mechanical surface-strengthening process, CIRP 46 (1) (1997) 113–116.
[13] S.R. Daniewicz, S.D. Cummings, Characterization of a water peening process, Transac. ASME: J. Eng., Mater. Technol. 121 (3) (1999) 336–340.
[14] B.M. Colosimo, M. Monno, Q. Semeraro, Process parameters control in water peening, Int. J. Mater. Product Technol. 15 (1/2) (2000) 10–19.
[15] M. Ramulu, S. Kunaporn, D. Arola, M. Hashish, H. Jordon, Waterjet machining and peening of metals, ASME J. Pressure Vessel Technol. 122 (1) (2000) 90–95.
[16] M. Ramulu, S. Kunaporn, M.G. Jenkins, M. Hashish, J. Hopkins, Peening with High Pressure Waterjets, SAE Technical Paper, 1999-01-2285, also to be published in SAE Transact.
[17] D.S. Hungerford, A.K. Hedley, E. Haberman, Total Hip Arthroplasty: A New Approach, University Park Press, Baltimore, MD, 1984, pp. 257–263.
[18] D. Arola, M.L. McCain, Abrasive waterjet peening: a new method of surface preparation for metal orthopedic implants, J. Biomed. Mater. Res.: Appl. Biomater. 53 (5) (2000) 536–546.
[19] I.C. Noyan, J.B. Cohen, Residual Stress. Measurement by Diffraction and Interpretation, Springer, Berlin, 1986.
[20] S. Amada, T. Hirose, T. Senda, Quantitative evaluation of residual grits under angled blasting, Surf. Coat. Technol. 111 (1) (1999) 1–9.
[21] B.J. Griffith, D.T. Gawne, G. Dong, A definition of the topography of grit blasted surfaces for plasma sprayed alumina coatings, ASME J. Manufact. Sci. Eng. 121 (1) (1999) 49–53.
[22] D. Arola, M. Ramulu, Material removal in abrasive waterjet machining of metals. Part I. Surface integrity and texture, Wear 210 (6) (1997) 50–58.
[23] D. Arola, M. Ramulu, Material removal in abrasive waterjet machining of metals: a residual stress analysis, Wear 211 (2) (1997) 302–310.
[24] H.K. Tonshoff, A. Mohlfeld, Surface treatment of cutting tool substrates, Int. J. Machine Tools Manufact. 38 (5/6) (1998) 469–476.